Materials and Structures, 1995, **28**, 586–595

Matrix design for pseudo-strain-hardening fibre reinforced cementitious composites

VICTOR C. LI, DHANADA K. MISHRA, HWAI-CHUNG WU

Advanced Civil Engineering Materials Research Laboratory, Department of Civil and Environmental Engineering, University of Michigan, Ann Arbor, MI 48109-2125, USA

while the composite elastic modulus is increased for all matrices with fine aggregates.

2. THEORETICAL DESIGN BACKGROUND

The parameters governing the behaviour of short fibre reinforced cement composites can be divided into three groups. The first consists of those related to fibre, such as fibre type, geometry and strength, etc., the second of matrix related parameters such as tensile strength, fracture toughness, elastic modulus, etc., and the third group consists of interface related parameters such as the interfacial bond strength. In this study only the effect of matrix parameters and the interfacial bond strength on composite pseudo-strain-hardening behaviour will be emphasized. It is important to understand the quantitative influence of these parameters on composite properties in order to select a suitable type of matrix.

2.1 Constraints for matrix toughness and interface bond

Based on the micromechanical theory of matrix crack extension and crack bridging by random discontinuous fibres, Li [4] shows that the fibre content must exceed a certain critical volume fraction V_f^{crit} for a brittle matrix composite to exhibit pseudo-strain-hardening under uniaxial tensile loading. This critical fibre volume fraction can be expressed in terms of fibre, matrix and interface parameters as follows:

$$V_f^{crit} \equiv \frac{12 J_c}{g\tau(L_f/d_f)\delta_0} \tag{1}$$

where J_c is the composite crack tip toughness, and L_f and d_f are fibre length and diameter, respectively. The snubbing factor g [5] and interface frictional bond strength τ are the parameters which describe the interaction between fibre and matrix. The snubbing factor can be interpreted physically as the increase in bridging force across a matrix crack when a fibre is pulled out at an inclined angle, analogous to a flexible rope passing over a friction pulley. Finally, δ_0 is the crack opening at which the fibre bridging stress reaches a maximum, σ_0, and is given by [5]:

$$\delta_0 = \frac{\tau L_f^2}{E_f d_f (1 + \eta)} \tag{2}$$

where $\eta = (V_f E_f)/(V_m E_m)$, and V_f, E_f are the fibre volume fraction and elastic modulus, respectively, and V_m, E_m are the matrix volume fraction and elastic modulus, respectively.

When a brittle matrix shows pseudo-strain-hardening, the ultimate strength of the composite σ_{cu} coincides with the maximum bridging stress σ_0, given by [5, 6]:

$$\sigma_{cu} = \tfrac{1}{2} g\tau V_f \left(\frac{L_f}{d_f}\right) \tag{3}$$

In Equation 1, the composite crack tip toughness can be related to the matrix fracture toughness K_m via [7]

$$J_c = \frac{K_m^2(1 - V_f)(1 - v_m^2)}{E_m} \tag{4}$$

where v_m is the matrix Poisson's ratio. The $(1 - V_f)$ factor takes into account the reduced crack front dimension due to the presence of fibres. For our purpose, since the fibre volume fraction is limited to a few per cent, this correction is relatively unimportant. For the same reason, the term η in equation 2 can be dropped. Further simplification can be obtained by approximating the $(1 - v_m^2)$ term as unity, so that

$$J_c = \frac{K_m^2}{E_m} \tag{5}$$

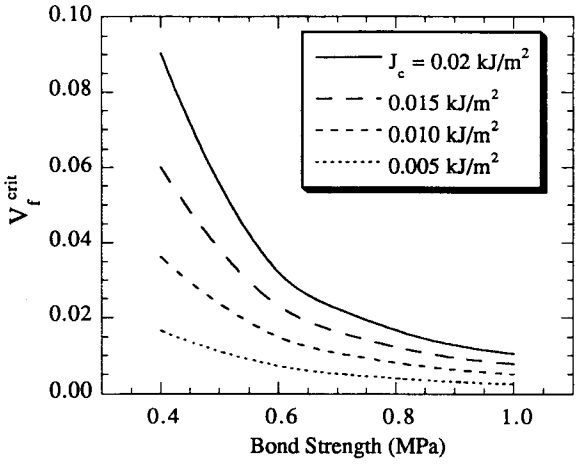

Fig. 2 Effect of matrix fracture toughness and interfacial bond strength on critical fibre volume fraction (E_f = 117 GPa, L_f = 12.7 mm, d_f = 0.038 mm, g = 2.0, E_m = 25 GPa).

Equation 1 is used to generate the design plot in Fig. 2 which shows the expected critical fibre volume fraction V_f^{crit} as a function of interface bond strength τ, for various values of J_c. In this research we have used a cement matrix ECC designed with a high modulus polyethylene fibre (trade name Spectra) as the base reference. Other matrices with controlled water and sand contents have been used to study their effect on composite behaviour. These modifications are expected to result in alterations in the value of J_c and τ. Direct pull-out test of Spectra fibre from a cement matrix has yielded τ = 0.5–0.6 MPa. This parameter can be tailored further by surface modification techniques such as plasma treatment [8]. The parametric values used for the Spectra fibre are given in the caption of Fig. 2.

2.2 Design guidelines

For the purpose of this investigation, based on the theoretical discussions presented above and with the help

of Fig. 2, we can derive the following three guidelines for desirable matrix properties:

1. With all other parameters being the same, the lower the matrix toughness J_c, the easier it is to achieve ductile behaviour of the composite. With fibre volume fraction in the practical range below 2%, the toughness of the matrix should be less than 0.01 kJ m^{-2} to ensure pseudo-strain-hardening, for a bond strength of 0.6 MPa or less. The fine aggregate content should be adjusted to achieve this upper limit for mortar matrix fracture toughness.
2. With all other parameters remaining the same, a higher bond strength will enhance composite performance in terms of composite strength (Equation 3) as well as reducing fibre volume necessary for strain hardening. The fibre–matrix interfacial bond strength should have a minimum value of 0.5 MPa. Plasma treatment of the Spectra fibre should be applied for interfacial bond enhancement.
3. A low first crack strength indicates a low fibre volume fraction requirement. This can be controlled either through matrix toughness and/or flaw size distribution. Since the flaw size is difficult to control quantitatively, for all practical purposes the tensile strength of the matrix is limited to 3.0 MPa. This value is chosen so that the composite first crack strength, assumed to be close to the matrix tensile strength, will be below the composite ultimate strength σ_{cu}, given by Equation 3.

Some of the micromechanical properties such as interfacial bond strength and first crack strength are affected simultaneously by mix parameters such as water/cement ratio, aggregate content, and fibre volume fraction. This presents some difficulty in independent control of each micromechanical parameter. As a result additional experimental measurements or theoretical interpretations of these parameters are needed.

3. EXPERIMENTAL PROCEDURE

The matrix properties such as the tensile strength, fracture toughness and elastic modulus are affected by many parameters such as water/cement ratio (w/c), sand/cement ratio (s/c), type of aggregate, type of cement, curing and so on. For the purpose of the current investigation w/c and s/c were identified as the most important factors in governing the matrix mechanical properties. An experimental program was designed with two purposes. One was to understand the effect of fine aggregates on matrix mechanical properties such as fracture toughness, tensile strength, compressive strength and elastic modulus. The second was to use one of the suitable matrix mixes thus studied to produce a new ECC, with aggregates, that will exhibit improved elastic modulus. It can be seen from the available literature that there have been very few experimental programs that have accounted for the different mechanical properties of the cement mortar mixes with a view to achieving a desirable combination of properties. However, many experimental studies have reported the influence of various mix parameters on a particular property of the material, such as compressive strength, elastic modulus or splitting tensile strength or fracture toughness [9–11]. The test procedures in compression, tension and fracture are described in the following sections.

3.1 Uniaxial compression test

The compression cylinders were tested in an Instron Model 8000 test system with a 2500 kN capacity loading frame. Each cylinder was capped with sulfur and tested under displacement control at a loading rate of 0.0254 mm s^{-1} (0.001 in s^{-1}). In the case of the plain matrix specimens (except for MR#5, see Section 4 for matrix material description) the failure load was noted and the compressive strength was calculated by dividing the failure load by the cross-sectional area of the cylinder. In the case of the fibre composites and MR#5, the complete load–deformation data were recorded. The deformation data were collected from the LVDT installed in the machine head as well as from strain gauges glued onto the specimens.

3.2 Uniaxial tension test

The tension coupon specimens were tested under displacement control in a 133.5 kN capacity MTS 810 material testing system with hydraulic wedge grips. The displacement rate used was 0.005 mm s^{-1}. For composite specimens the tensile specimen set-up is as shown in Fig. 3a. Aluminium plates were glued onto the ends of the tension specimens to facilitate gripping. The MTS machine has a fully digital control panel. In addition, two LVDTs were used to measure displacements between two points on the specimen at a gauge length of 205 mm. The tensile behaviour can then be determined from these tests. In the case of the matrix specimens thin sheets of lead were used for frictional gripping. Only the tensile strength was recorded for the matrix specimen. The loading rate used for the plain matrix specimen and the elastic portion of the composite specimen was 0.001 mm s^{-1}, whereas the speed was increased up to 0.05 mm s^{-1} in steps for the strain hardening regime of the composite tests. The tensile testing procedure is described in greater detail elsewhere [12].

3.3 Compact tension fracture test

The compact tension specimen as illustrated in Fig. 3b, was used to determine the fracture toughness of the matrix material following a procedure similar to that described in ASTM E 399-78. According to this procedure, for the compact tension specimen geometry used the conditional fracture toughness is given by

$$K_Q = (P_Q/BW^{1/2})f\left(\frac{a}{W}\right)$$

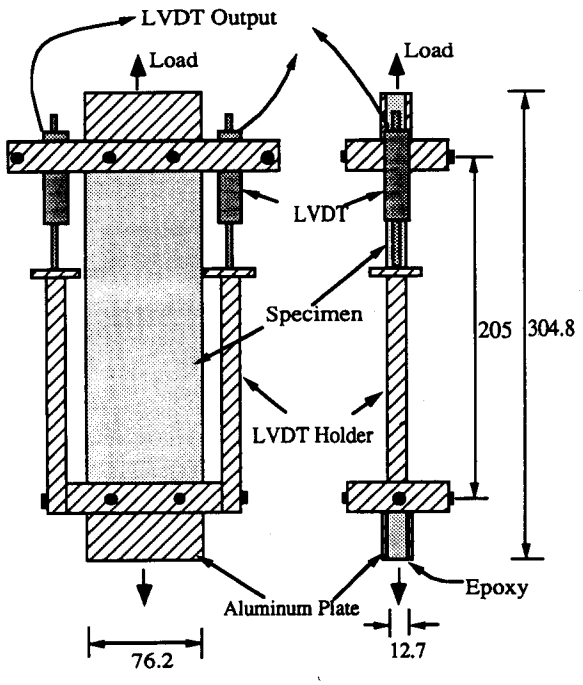

(a)

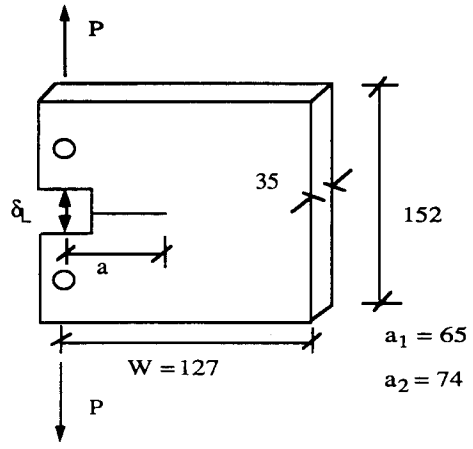

(b)

Fig. 3. (a) Schematic diagram of the tension test set-up, and (b) the dimensions of the compact tension specimen (all dimensions in mm).

where

$$f\left(\frac{a}{W}\right) = \frac{\left(2+\frac{a}{W}\right)\left(0.886+4.64\left(\frac{a}{W}\right)-13.32\left(\frac{a}{W}\right)^2+14.72\left(\frac{a}{W}\right)^3-5.6\left(\frac{a}{W}\right)^4\right)}{\left(1-4.64\left(\frac{a}{W}\right)\right)^{3/2}} \quad (6)$$

with P_Q the lowest load at which significant crack extension occurs (not less than 90% of P_{max}) determined as per the provisions of the ASTM E 399-78, B the specimen thickness, W the specimen width, and a the crack length.

The dimensions of the specimen used in this study are shown in Fig. 3. For K_m as measured by the LEFM method to be valid, the fracture process zone size should be small compared with all relevant specimen dimensions. Using the concept of material characteristic length ($l_{ch} = (K_{IC}/f_t)^2$, where f_t is the matrix tensile strength), as proposed by Hillerborg [13], Li and Liang [14], showed that laboratory size specimens are inadequate for fracture resistance measurement for materials having large critical crack opening in their stress–separation curves as in concrete and FRC. However, in cases of cement paste and mortar (maximum aggregate size < 1 mm) the measured fracture toughness based on LEFM appears to be more reliable. The sand used in the present experiments has a maximum particle size of less than 0.3 mm. The average characteristic length calculated from these tests is in the range 20–50 mm, which is of the same order of magnitude as the least planar dimension of the specimen. According to the numerical calculations of Li and Liang [14], the maximum error generated in estimating K_m due to the small scale yielding assumption in LEFM should be less than 10% for the matrix materials used in the present experiment. Also the spread of the data is in the range of 20% around the mean. Although these fracture data are generally consistent with expected trends, they should be regarded as approximate values only.

All compact tension specimens were tested in the same machine as that used for the tension test using special gripping fixtures. All tests were carried out under displacement control at a loading rate of 0.001 mm s^{-1} such that the entire test takes less than 5 min.

3.4 Measurement of elastic modulus of composites

Wire type bonded electrical strain gauges (20 mm in length, manufactured by TML Corporation of Japan) were used to measure the elastic modulus of the composites. The modulus in both tension and compression of the composites used in this study were measured. Standard surface preparation and strain gauging procedures were used. For tension plates two parallel strain gauges were used on one face of the specimen at the centre of the gauge length, and for compression cylinders two vertical strain gauges on opposite sides were used to measure the elastic modulus.

4. MATRIX COMPOSITION AND PREPARATION

One of the bases for the selection of some of the matrix mix compositions used in this program is shown in Fig. 4. It shows the effect of s/c on matrix elastic modulus for different w/c. These predictions are based on a model proposed by Hasin [15]. According to this model, the elastic modulus of a two-phase heterogeneous material such as cement mortar (the two phases being cement paste and sand) can be expressed in terms of the elastic

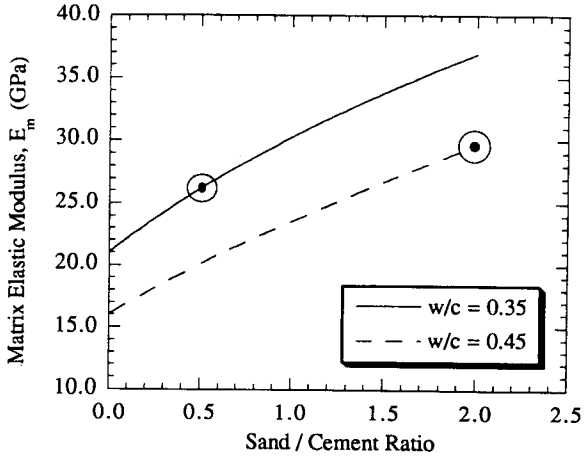

Fig. 4 Effect of s/c and w/c on matrix elastic modulus at age 28 days: the points in circles indicate the matrix chosen for mixes II and III.

moduli of the sand and the cement paste as follows:

$$E_m = \left[\frac{(1 + V_a)E_a + (1 - V_a)E_p}{(1 - V_a)E_a + (1 + V_a)E_p}\right]E_p \qquad (7)$$

where E_m is the elastic modulus of the matrix (to be used in the fibre composite), E_p, $V_p(= 1 - V_a)$ and E_a, V_a are the elastic modulus and volume fraction of the paste and aggregate respectively. In this derivation the Poisson's ratios of both phases and the composite have been assumed to be 0.2 for cementitious matrix material. A value of 72 GPa has been assumed for the elastic modulus of the silica sand used in the present investigation [16]. The elastic modulus of the paste for a given w/c ratio and age has been obtained from the experimental data provided by Hirsch [11]. As can be observed later on, the use of small quantities of sand can increase the elastic modulus of the matrix substantially over that of the cement paste. The above equation thus serves as a guide for the selection of a particular matrix to achieve a certain composite elastic modulus.

The mix compositions of all the matrix mixes (MR#1–MR#7) used in this study are listed in Table 1. MR#1 is a cement paste matrix without aggregates that has been used in the program for comparison purposes. Two values of w/c ratio (0.35 and 0.45) and three values of s/c ratio (0.5, 1.0 and 2.0) have been used. Type I Portland cement and silica sand were used in all cases. A type F-100 silica fume supplied by Elkem is used in all mixes. The sand used is graded silica sand conforming to ASTM C 50-70 (uniformly graded between particle sizes 0.3 mm and 0.15 mm corresponding to ASTM sieves #50 and #70). A small amount of superplasticizer (melamine) was used to adjust workability whenever necessary. Figure 4 shows the estimated elastic modulus of each of these matrix mixes as per Eq. (7). The two matrix mixes (MR#4 and 5) subsequently used in composite mixes II and IIIa, b are indicated in circles in Fig. 4.

The matrix is carefully prepared in a Hobart mixer. For each of the matrix mixes at least three specimens

Table 1 Matrix mix proportions

Mix designation	Cement	SF[a]	Sand	w/c^b
MR#1[c]	1.0	0.2	0.0	0.32
MR#2	1.0	0.2	0.5	0.45
MR#3	1.0	0.2	1.0	0.45
MR#4[d]	1.0	0.2	2.0	0.45
MR#5[e]	1.0	0.2	0.5	0.35
MR#6	1.0	0.2	1.0	0.35
MR#7	1.0	0.2	2.0	0.35

[a] SF = silica fume
[b] w/c = water to cement ratio.
[c] Cement paste used in composite mix U.
[d] Matrix mix used in composite mix II.
[e] Matrix mix used in composite mix III.

each of tension plates (305 mm × 76 mm × 13 mm), compression cylinders (152 mm × 76 mm) and compact tension specimens (152 mm × 152 mm × 35 mm) were cast from the same batch of materials.

All specimens were demolded after one day of moist curing under plastic sheets and placed into water curing tanks at room temperature for four weeks. All specimens were approximately four to five weeks old at testing, and were under visually dry conditions at the time of the test.

5. MATRIX PROPERTIES

The matrix test results are listed in Table 2. The average measured compressive strength f'_c, tensile strength f_t and matrix fracture toughness K_m of each mix are listed. The composite crack tip toughness J_c has been calculated as per Equation 5. The elastic modulus of the matrix has been estimated using Equation 7. As a check, the prediction for matrix MR#5 (26.2 GPa) is compared with the measured elastic modulus (24.7 GPa) of the matrix. Reasonable correspondence with the prediction in this case gives confidence in the predicted modulus of the other matrices. In the following sections these matrix properties are analysed from the point of view of the effect of w/c and s/c on the tensile strength and the fracture toughness of the material.

5.1 Effect of water/cement ratio

Figs 5 and 6 show the effect of w/c on the tensile strength and matrix fracture toughness, respectively, for a variety of s/c ratios. Since all the mixes contain the same amount of silica fume (20% by weight), the water to cementitious ratio is 83% of the w/c figure. It can be observed that a decrease in w/c from 0.45 to 0.35 results in an increase in both properties at all sand/cement ratios, although the difference appears to diminish at high s/c ratios. For example, for the matrix with $s/c = 1.0$, there is an increase of 29% in tensile strength and 73% in toughness. This large increase in toughness makes it difficult to use this matrix and still ensure strain-hardening behaviour in the

Table 2 Matrix test results

Mix	f'_c, Comp. strength (MPa)	f_t, Tensile strength (MPa)	K_m, Fracture toughness (MPa $m^{1/2}$)	E_m, Elastic modulus of matrix (GPa)[a]	J_c, Composite crack tip toughness (kJ m^{-2})[b]
MR#1	45.0	1.60	0.33	23.0	0.0047
MR#2	61.3	1.90	0.31	20.1	0.0048
MR#3	65.7	2.40	0.41	23.6	0.0070
MR#4	82.5	3.20	0.57	30.7	0.0108
MR#5	78.2	2.95	0.38	26.2	0.0055
MR#6	90.6	3.15	0.71	30.3	0.0168
MR#7	90.8	3.30	0.66	36.9	0.0118

[a] Following [15].
[b] Following Equation 5.

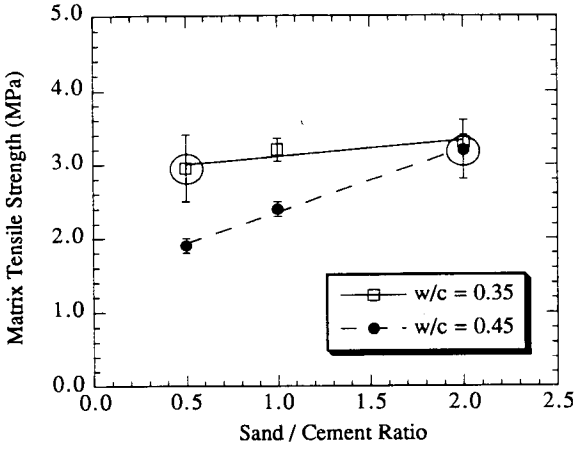

Fig. 5 Effect of s/c and w/c on matrix tensile strength.

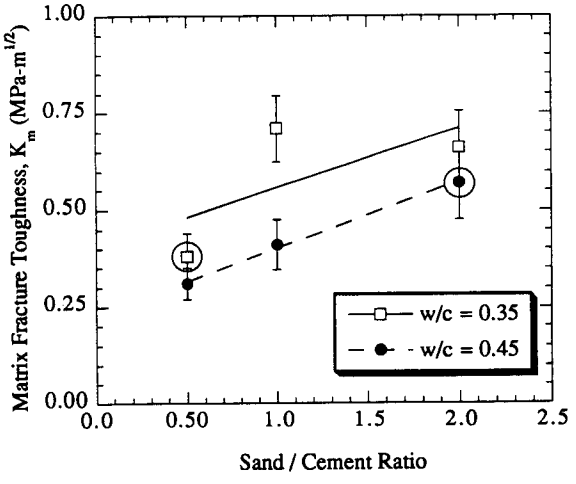

Fig. 6 Effect of s/c and w/c on matrix fracture toughness.

composite, Thus, the effect of w/c is very important in choosing a matrix for the composite.

5.2 Effect of sand/cement ratio

Figs 5 and 6 also show that the effect of addition of fine aggregates is to increase the fracture toughness and the tensile strength for a given w/c. It can be observed that at a constant w/c of 0.45, the tensile strength goes up by 33% for an increase in s/c from 1.0 to 2.0. Similarly, the fracture toughness goes up by 39% for a similar change in sand content. These results suggest that the sand content must be limited in the matrix mix for the design of a strain hardening composite. However, for a w/c of 0.35 a decrease in K_m is observed for a higher s/c. This could be due to the higher porosity introduced due to presence of a large amount of sand when w/c is low.

6. COMPOSITE DESIGN

Table 3 shows the mix compositions of the composite mixes tested so far. For comparison purposes we have listed the ECC mix without aggregates as mix I. This ECC material has exhibited very high ductility but with relatively low elastic modulus (20.3 GPa). The matrix MR#4 was chosen for composite mix II for its high elastic modulus (30.7 GPa). The matrix MR#5 was chosen for composite mix III for its lower fracture toughness with modulus (26.2 GPa) moderately higher than that of mix I. For both MR#4 and MR#5, the tensile strength is close to 3 MPa. In all cases the fibre used is a high modulus polyethylene fibre (trade name Spectra-900 fibre). The fibre length is 12.7 mm and diameter 38 μm. It has an elastic modulus of 117 GPa and specific gravity of 0.97. The fibre volume fraction used in each case was fixed at 2%. Two batches of tensile specimens were tested for mix III. One used fibres without

Table 3 Composite mix proportions

Mix designation	Cement	SF	Sand	SP[a]	w/c	Fibre[b]
Mix I	1.0	0.2	0.0	0.03	0.32	0.02
Mix II	1.0	0.2	2.0	0.05	0.45	0.02
Mix III	1.0	0.2	0.5	0.05	0.35	0.02

[a] SP = superplasticizer.
[b] Volume fraction.

Table 4 Composite test results

Mix designation	f'_c, Comp. strength (MPa)	σ_{cu}, Tensile strength (MPa)	Strain capacity (%)	Deduced interfacial bond strength (MPa)	Average elastic modulus (GPa)
Mix I	65.6	4.7	5.60	0.70	20.3
Mix II	72.2	2.9	0.24	0.43	28.3
Mix IIIa	55.7	3.5	1.70	0.52	26.0
Mix IIIb	55.7[a]	4.8	3.80	0.72	26.0[a]

[a] Assumed same as Mix IIIa.

plasma treatment (called mix IIIa) and the other used plasma treated fibres (called mix IIIb). Plasma treatment was found to provide about 100% improvement in bond strength of the polyethylene fibre [8]. However, the actual bond property is not known beforehand for composite mixes II, IIIa and IIIb. A more complete experimental program would include measurement of this important property by single fibre pull-out test.

The fibres were added manually as the prepared matrix was mixed at a slow speed. To ensure proper distribution the fibres must be added slowly over a period of about 10 min. The casting of ECC material was carried out using high frequency vibration (80–120 Hz). The workability of the mix has been designed to be such that segregation or bleeding is avoided in spite of the use of high frequency vibration. Further details on specimen preparation can be found in [12]. At least three tensile specimens and compression specimens were cast.

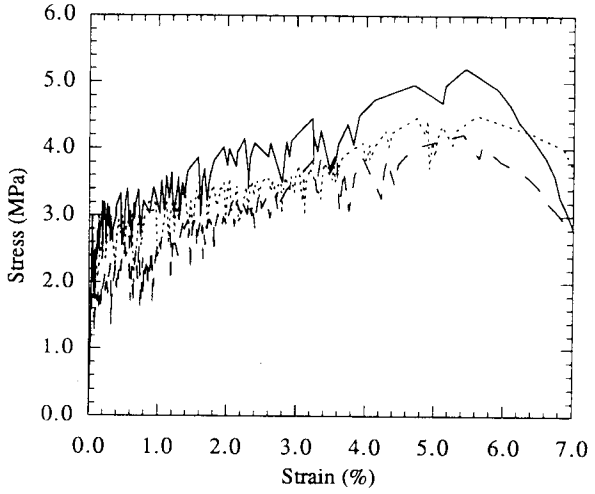

Fig. 7 Tensile stress–strain behaviour of composite mix I at age 28 days.

7. COMPOSITE PROPERTIES

The test results of the composites are summarized in Table 4. The interfacial bond strength values were deduced using Equation 3. The elastic modulus is the average value of those measured in both tension and compression. Composite mixes IIIa and IIIb produced substantial strain hardening behaviour, whereas mix II behaved more like an ordinary fibre reinforced composite. Composite mixes I and IIIa were tested in both tension and compression.

7.1 Tensile strength and strain capacity

Fig. 7 shows the tensile stress–strain behaviour of a typical ECC composite without aggregate. Similarly, Fig. 8 shows the tensile behaviour of composite mix II, characterized by the typical strain softening behaviour of ordinary fibre reinforced concretes (FRC). Figs 9 and 10 show the tensile behaviour of a typical composite mix III material. The tensile strength of mix IIIa (3.5 MPa) is about 35% lower than that of mix I (4.7 MPa), whereas that of IIIb (4.8 MPa) is 2% higher. This shows the effect of plasma treatment, which is also reflected in the bond strength values. The tensile strain capacities of mixes I and IIIb are of the same order (5.6% versus 3.8%) which

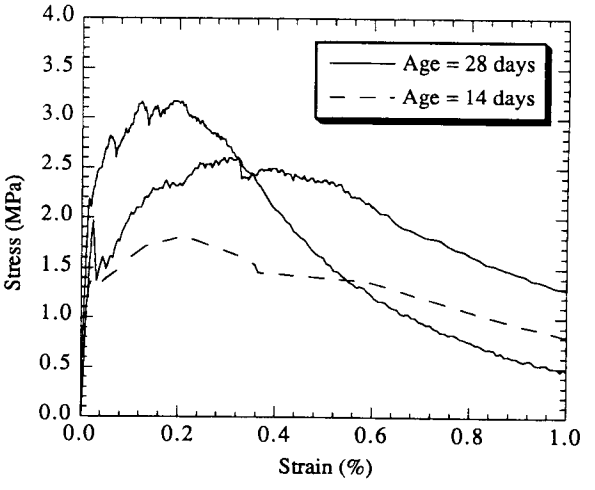

Fig. 8 Tensile stress–strain behaviour of composite mix II.

is an order of magnitude higher than that of mix II (0.24%). Fig. 11 shows the typical stress–strain behaviour of the four composites together for comparison. The graphs have been smoothed for clarity. It demonstrates that ECC materials with improved elastic modulus can be designed that still maintains their ductility, provided the amount of fine aggregates is properly controlled.

In Fig. 12, the matrix toughness is plotted against the

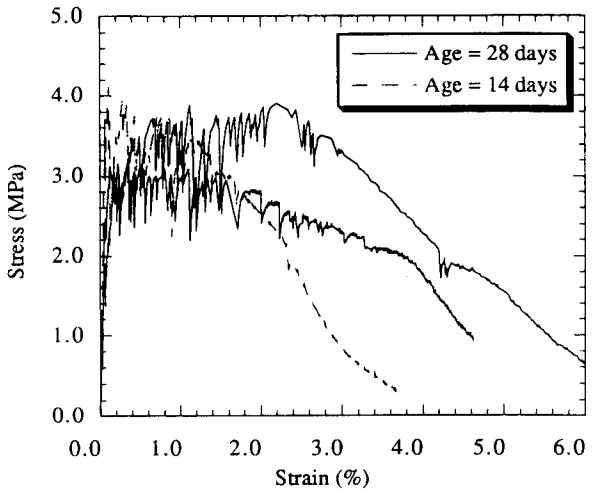

Fig. 9 Tensile stress–strain behaviour of composite mix IIIa (without plasma treatment).

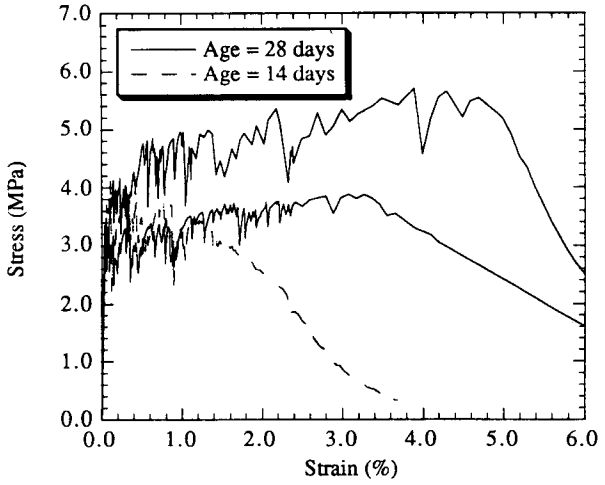

Fig. 10 Tensile stress–strain behaviour of composite mix IIIb (with plasma treatment).

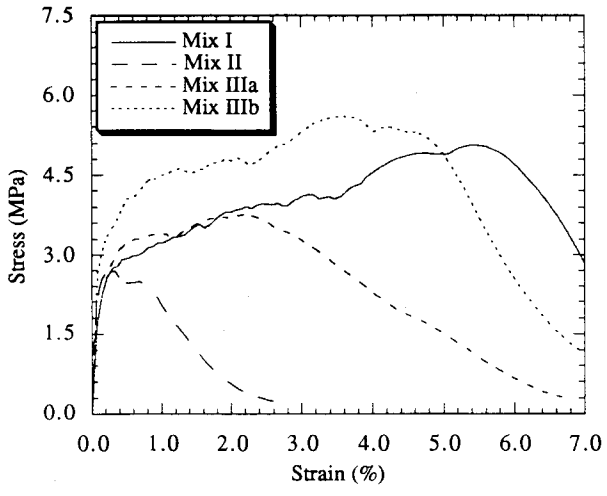

Fig. 11 Comparison of tensile stress–strain behaviour of various composites.

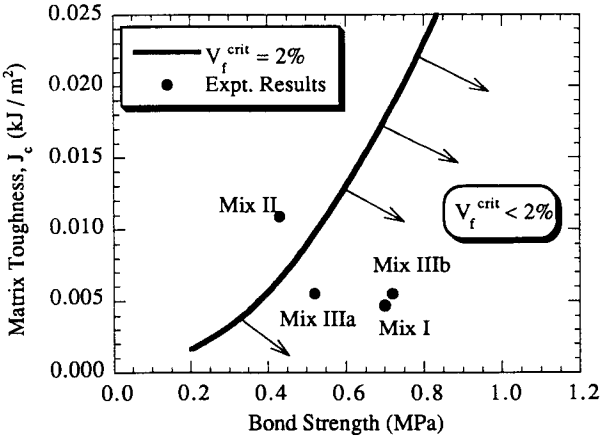

Fig. 12 Variation of matrix fracture toughness with interfacial bond strength and critical fibre volume fraction (E_f = 117 GPa, L_f = 12.7 mm, d_f = 0.038 mm, g = 2.0, E_m = 25 GPa).

interface bond strength for a fixed critical fibre volume fraction of 2%, based on Equation 1. This curve separates the strain hardening and quasi-brittle failure modes for composites with $V_f = 2\%$. All combinations of (τ, J_c) to the left of this curve correspond to composites expected to show quasi-brittle behaviour. On the other hand, all combinations of (τ, J_c) to the right of the curve correspond to composites expected to show pseudo-strain-hardening. The composite experimental results in terms of its estimated interfacial bond strength τ and matrix toughness J_c are plotted as filled circles. The matrix toughness has been estimated using Equation 5 and the measured K_m values and estimated E_m values listed in Table 3. It can be seen that mixes I, IIIa and IIIb do fall in the region of pseudo-strain-hardening, whereas mix II does not. This is consistent with our strain-capacity observations (Fig. 11) from the composite tensile tests described earlier.

In the case of mix IIIa which uses the matrix MR#5, the composite ultimate tensile strength is almost 62% higher than the matrix strength, which further confirms the occurrence of pseudo-strain-hardening. For the measured values of matrix fracture toughness, tensile strength, elastic modulus and deduced bond strength, theoretical calculations show that the fibre volume fraction required for ensuring matrix multiple cracking is 1.5–2% for mix IIIa. However, if the interfacial bond strength is increased from 0.52 MPa to 0.72 MPa (as was achieved by plasma treatment in mix IIIb), the fibre volume fraction required decreases to the range 0.5–1.0%. The fact that substantial pseudo-strain-hardening was achieved using only 2% fibre in each case reveals experimental consistency with theoretical predictions.

7.2 Compressive strength

The average compressive strengths of each of the composite mixes used in the study are listed in Table 4. It can be observed that the compressive strength of composite mix IIIa is rather low compared with its corresponding matrix (55.7 MPa versus 78.2 MPa). This

could be due to a fibre induced damage effect, which results in a composite with higher porosity compared with the matrix material alone [17]. The behaviour of composite mixes I and IIIa is very similar. Mix II yields the highest compressive strength (72.2 MPa) as it has the highest sand content. The fact that mix I without aggregate has a higher average compressive strength (65.6 MPa) compared with mix IIIa with aggregates may be due to the difference in w/c (0.32 versus 0.35). Mix IIIb has not been tested in compression as the only difference between mixes IIIb and IIIa is the plasma treated fibres. Li and Mishra [17] have shown theoretically that interfacial bond strength enhancement (such as due to plasma treatment) can increase the compressive strength of the composite. This remains to be established experimentally.

7.3 Elastic modulus

For the purpose of this investigation the elastic modulus of the composite is defined as the slope of the initial linear portion of the stress–strain response in both tension and compression. The strain measured by the bonded electrical strain gauges were used for calculating the elastic modulus. Only selected compression and tension specimens (a minimum of two each) of the composite mixes were used for modulus measurement. The elastic modulus values found are listed in Table 4, and those of the composites are in general lower than the calculated elastic moduli of the corresponding matrix materials.

The elastic modulus of composite mix IIIa is about 28% higher than that of composite mix I. This is a substantial gain considering that only a small amount of aggregate has been used. The modulus of mix IIIb can be assumed to be same as that of mix IIIa as the only difference between the two composite is in the bond strength. The modulus of mix II (28.3 GPa) is only slightly higher than that of mix IIIa (26.0 GPa). This indicates that the trade-off between elastic modulus and tensile strain capacity may be such that it is of little advantage to increase the sand content by a large amount over that used in mixes IIIa/IIIb for the given fibre system used in this study.

7.4 Fibre–matrix bond strength

In addition to matrix fracture toughness, frictional bond strength τ is another important microparameter which governs the tensile behaviour of fibre reinforced composites (see Equations 1 and 3). The bond strength can be deduced from the composite ultimate strength in the case where the composite strength exceeds the first crack strength of the matrix (Equation 3). These deduced bond strengths are listed in Table 4. A weak dependence of bond strength on both w/c and s/c is observed. The presence of sand and increase in w/c tend to reduce the interfacial bond. The bond strength between polyethylene fibre and mortar matrix can be taken as 0.5 MPa, at least for all systems used in this study. An increase of 40% is observed as a result of plasma treatment. Enhanced bond strength through various fibre surface modifications such as plasma treatment and addition of coupling agent is discussed elsewhere [8, 12].

8. CONCLUSIONS AND FURTHER DISCUSSIONS

This paper presents results of experimental research on the effect of fine aggregates on the pseudo-strain-hardening behaviour of fibre reinforced cementitious composites. It is found that while fine aggregates improve composite elastic modulus in all cases, excessive use of fine aggregates can lead to a suppression of desirable pseudo-strain-hardening behaviour and accompanying material ductility in tension. This finding is consistent with theoretical calculations based on micromechanics which relate a critical fibre volume fraction to matrix toughness and interface bond property. The experimentally determined higher matrix toughness resulting from fine aggregate addition leads to a higher critical fibre volume fraction. A decrease in water/cement ratio also appears to have a similar effect. On the other hand, enhanced bond properties by fibre surface modification leads to a lower critical fibre volume fraction. As a result, engineered cementitious composites with fine aggregates and higher elastic modulus can still maintain their ductility via pseudo-strain-hardening, as long as the matrix toughness is controlled properly and the interface bond tailored properly.

The use of the micromechanical model, combined with experimental correlation between matrix toughness and matrix constituents (w/c and s/c studied here), can be a very powerful tool for composite design. While this work emphasizes matrix property control, it is equally important in tailoring the fibre and interface properties for composite design. These aspects are addressed in other publications [8, 12].

ACKNOWLEDGMENTS

The research reported here has been supported by grants from the National Science Foundation to the University of Michigan. Additional support has been received from the Shimizu Corporation, Tokyo, Japan. Special thanks are due to Drs. T. Fujimori, Y. Inada, Y. Kaneko, and to Mr. T. Yagi.

REFERENCES

1. Aveston, J., Cooper, G. A. and Kelly, A., 'Single and multiple fracture', in 'Properties of Fiber Composites' (IPC Science and Technology Press Ltd., Guildford, UK, 1971) pp. 15–24.
2. Li, V. C. and Wu, H. C., 'Conditions for pseudo strain-hardening in fiber reinforced brittle matrix composites', *Appl. Mechn. Rev.* **45** (1992) 390–398.

3. Li, V. C. and Leung, C. K. Y., 'Theory of steady state and multiple cracking of random discontinuous fiber reinforced brittle matrix composites', *ASCE J. Engng Mech.* **118** (1992) 2246–2264.
4. Li, V. C., 'From micromechanics to structural engineering—The design of cementitious composites for civil engineering applications', *J. Struct. Mech. Earthquake Engng* **10** (1993) 37–48.
5. Li, V. C., Wang, Y. and Backer, S., 'Effect of inclining angle, bundling, and surface treatment on synthetic fiber pull-out from a cement matrix', *Composites* **21** (1990) 132–140.
6. Li, V. C., 'Post crack scaling relations for fiber reinforced cementitious composites', *ASCE J. Mater. Civil Engng* **4** (1992) 41–57.
7. Budiansky, B. and Cui, Y. L. 'On the tensile strength of a fiber-reinforced ceramic composite containing a crack-like flaw', *J. Mech. Phys. Solids* **42** (1994) 1–19.
8. Li, V. C., Wu, H. C. and Chan, Y. W., 'Interfacial property tailoring for pseudo strain-hardening cementitious composites', in 'Advanced Technology on Design and Fabrication of Composite Materials and Structures', edited by Carpinteri and Sih (Kluwer, Dordrecht, 1995) pp. 261–268.
9. Naus, D. J. and Lott. J. L., 'Fracture toughness of Portland cement concretes', *J. Amer. Concr. Inst.* **66** (1969) 481–489.
10. Higgins, D. D. and Bailey, J. E., 'Fracture measurement on cement paste', *J. Mater. Sci.* **11** (1976) 1995–2003.
11. Hirsch, T. J., 'Modulus of elasticity of concrete affected by elastic moduli of cement paste matrix and aggregate', *J. Amer. Concr. Inst.* **59** (1962) 427–451.
12. Li, V. C., Wu, H. C., Maalej, M. M., Mishra, D. K. and Hashida, T., 'Tensile behavior of engineered cementitious composites with discontinuous random steel fibers', *J. Amer. Ceram. Soc.* (1995), in press.
13. Hillerborg, A., 'Analysis of one single crack', in 'Fracture Mechanics of Concrete', edited by F. H. Wittmann (Elsevier, Amsterdam, 1983) pp. 223–249.
14. Li, V. C. and Liang, E., 'Fracture processes in concrete and fiber reinforced cementitious composites', *J. Engng Mech.* **112** (1986) 566–586.
15. Hasin, Z., 'The elastic moduli of heterogeneous material', *J. Appl. Mech. Trans. ASME* **29** (1962) 143–150.
16. Lide, D. R., 'CRC Handbook of Chemistry and Physics' (CRC Press, Boca Raton, 1991).
17. Li, V. C. and Mishra, D. K., 'Micromechanics of fiber effect on the uniaxial compressive strength of cementitious composites', in 'Fiber Reinforced Cement and Concrete', Proceedings of the 4th RILEM International Symposium, Sheffield, U.K., edited by R. N. Swamy (1992) pp. 400–414.

RESUME

Conception de la matrice pour le pseudo-écrouissage de composites cimentaires renforcés de fibres

Au cours de ces dernières années, on a démontré de façon expérimentale le comportement de pseudo-écrouissage sous charge en traction directe de composites cimentaires renforcés de fibres courtes calculés à l'aide des données quantitatives de la micromécanique. Les conditions déterminant le comportement ductile de ces composites (ECC) ont été formulées de façon théorique. Dans cet article, on insiste particulièrement sur l'influence des propriétés de la matrice sur le pseudo-écrouissage du composite. On a entrepris un programme d'essais dans le but de déterminer l'influence de la composition des mélanges régis par les rapports eau/ciment et sable/ciment sur les propriétés de la matrice. La combinaison des savoirs théorique et expérimental ainsi obtenus permet de proposer une procédure innovante concernant le calcul des composites avec différents types de matrice. Cette étude résulte de la nécessité de mettre au point une nouvelle classe d'ECC présentant un module d'élasticité amélioré par l'addition de granulats fins à la matrice cimentaire. Enfin, on calcule un nouveau composite dont les essais montrent qu'il présente les caractéristiques souhaitables de comportement au pseudo-écrouissage et d'amélioration du module d'élasticité.